Theoretical study of dislocation nucleation from simple surface defects in semiconductors

J. Godet,* L. Pizzagalli, S. Brochard, and P. Beauchamp
Laboratoire de Métallurgie Physique, CNRS UMR 6630, Université de Poitiers, B.P. 30179, 86962 Futuroscope Chasseneuil Cedex, France
(Dated: February 1, 2008)

dislocation nucleation

PACS numbers: pacs codes
Keywords: dislocation; nucleation; silicon; simulation

I. INTRODUCTION

The plasticity of semiconductors has been a subject of numerous studies for the last decades in both fundamental and applied research. Despite significant progress in the understanding of the fundamental mechanisms involved, several issues remain, in particular for nanostructured semiconductors. In these materials, including for example nano-grained systems or nanolayers in heteroepitaxy, dimensions are usually too small to allow the classical mechanisms of dislocation multiplication, such as Franck-Read sources.[1] It is then likely that other mechanisms dominate, and it has been already proposed that surfaces and interfaces, which become prominent for small dimensions, play a major role. Several observations support this assumption, especially for strained layers and misfit dislocations at interfaces.[2,3,4] The question of dislocation formation at surfaces concerns also bulk materials submitted to large stresses.[5,6,7] The propagation of dislocation from surfaces has been investigated in the frame of a continuum model and elasticity theory. However, the characterization of the nucleation of dislocations is out of the reach of this approach, and the predicted activation energy is very large, in disagreement with experiments. It is also difficult to investigate experimentally the very first stages of dislocation formation. Hence, the mechanisms involved in the nucleation of dislocations from surfaces or interfaces are far to be well understood. There has been some attempts to perform atomistic calculations for addressing this issue. In particular, the interaction between a dislocation and the free surface or the interface,[8,9] or between ledges and a crack tip,[10] and the instability of a stressed ledge[11] have been studied.

It has been proposed that surface defects like steps, or cleavage ledges, could favor the nucleation of dislocations, by lowering the activation energy.[12] This assumption is supported by experimental facts, with dislocation sources located on the cleavage surface and coinciding with cleavage ledges.[13,14] Atomistic simulations of dislocation nucleation from surface defects in metals have also been recently reported.[15] It has been shown that the presence of the step modifies the otherwise uniform strain field,[16] which effectively makes easier the dislocation formation. The situation appears to be different for semiconductors, with no clear strain inhomogeneity at the step.[17,18] The role of the stress orientation on the dislocation formation is also unclear. Additional atomistic simulations are needed to shed light on these points and fully characterize the mechanisms behind dislocation nucleation.

In this paper, we report large-scale atomistic calculations of the nucleation of dislocations from surface defects in systems submitted to a stress with variable orientation. We focused on linear surface defects, with simple steps but also cleavage ledges. As for the material, silicon was selected as the best candidate, for several reasons. First, it is a good model, since a lot of semiconductors crystallize in the same cubic diamond structure, or the zinc-blende structure, almost equivalent from the point of view of plasticity. Second, silicon can be grown without dislocations, which allows a comparison between experiments and simulations. Finally, several high quality atomistic potentials are available. In the first part of the paper, the silicon structure and the slip systems are briefly described. After the presentation of the model and the calculations techniques used to perform the simulations, the results obtained with several empirical potentials are described. In particular, we mostly focus on stress orientations that increase the probability of nucleating the relevant dislocations. Several points are then discussed, such as the conditions of nucleation, the role of stress orientation and temperature, and the slip system selected.

II. METHODOLOGY

A. Structure and geometry

In ambient conditions, the stable structure of silicon is diamond cubic. Dislocations glide in the (111) dense planes, that are gathered together in two sets, one widely spaced, called "shuffle" set and one narrowly spaced, called "glide" set (Fig. 1a). The Burgers vector of a perfect dislocation is $1/2 < 1\bar{1}0 >$. Dissociation only occurs in the glide set, with two Shockley partial dislocations, $1/6 < 1\bar{2}1 >$ and $1/6 < 2\bar{1}\bar{1} >$.[19] Note that, since the Burgers vector of a partial dislocation doesn't join two points of the crystal lattice, the nucleation of a partial

dislocation is always accompanied by a stacking fault of the atomic plane. When occurring on adjacent atomic planes, the stacking faults form micro-twins. Considering the angle between the dislocation line and the Burgers vector, perfect dislocation are called 60° or screw, while partials are called 90° or 30°. These notations are used in the following.

A semi infinite system including surface steps is modeled by employing a slab with a 2×1 rebuilt (100) free surface (Fig. 2).[20,21] Four atomic layers are frozen in the bottom of the slab, opposite to the free surface. Steps, lying along the $[0\bar{1}1]$ dense directions, which correspond to the intersection of {111} slip planes and the (100) surface, are placed on the free surface. The steps are made infinite through the use of periodic boundary conditions along the [011] direction. Two steps of opposite signs are introduced in order to allow the use of periodic boundary conditions in the $[0\bar{1}1]$ direction normal to the step line. The dimensions along [100] and [011] have been determined by several calculations on systems with different sizes, for minimizing the interactions between the surface and the frozen bottom, and between steps (Fig. 2). A typical system encompasses 4 atomic layers along the step line direction $[0\bar{1}1]$, 120 along the surface normal [100] and 160 along [011], the normal to the step in the surface plane, i.e. about 80000 atoms.

Note that the periodicity of 4 atomic layers along the step direction is a severe limitation of the simulation in that it almost restricts the problem to two dimensions, and prevents in particular the formation and expansion of such defects as dislocation half-loops.

In this work, the most simple steps formed by the emergence of a perfect dislocation at the surface are considered. They are called D_B re-bonded and D_B non re-bonded,[22] and have a height of two atomic layers. The effect of higher steps is also checked by considering cleavage ledges corresponding to 5 D_B step forming a {111} facet.

B. Application of a uniaxial stress

To simulate the effect of an applied uniaxial stress $\boldsymbol{\sigma}$, the system is deformed with strains calculated using the silicon compliances S_{ijkl}. The latter are obtained from the elastic constants C_{ijkl}, computed for all empirical potentials. In this work, the uniaxial stress direction is contained into the surface, but its orientation with respect to the step line, can vary. As a result, the projection of this stress in the {111} slip planes, called the resolved shear stress, will also vary. This quantity is important since it is reasonable to assume that the slip system with the largest resolved shear stress along the Burgers vector $\mathbf{b}$ will be favored. The relationship between the resolved shear stress $\boldsymbol{\tau}$ and the uniaxial stress $\boldsymbol{\sigma}$ is $|\boldsymbol{\tau}| = \pm s|\boldsymbol{\sigma}|$, $s = cos\varphi\ cos\nu$ being the Schmid factor. φ is the angle between $\boldsymbol{\sigma}$ and the normal of the slip plane and ν the one between $\boldsymbol{\sigma}$ and $\mathbf{b}$. In the Fig. 3, the calculated Schmid factors along several slip directions into the {111} slip planes are represented as a function of the angle α between the stress orientation and [011], the normal to the step lines. Four dislocations are possible: the 60° and screw perfect dislocations, and the 90° and 30° partials. The most efficient stress orientations for each dislocation are gathered in the Fig. 1b. The maximum resolved shear stress along the Burgers vector of the 60° (screw) is obtained for $\alpha = 22.5°(45°)$ for both tensile and compressive stress, respectively. The 90° is favored in case of a non disorientated tensile stress only. A compressive stress would give a resolved shear stress in the anti-twinning sense. Finally, the 30° is favored by a disorientated stress of 36°, only in compression to produce a twinning stress.

C. Computational methods

The large number of atoms required in the simulation prevents the use of ab initio methods because it would be too expensive in CPU time. Instead, three classical potentials for silicon are employed: the potential of Stillinger and Weber (SW),[23] based on a linear combination of two- and three-body terms, the Tersoff potential[24] including many-body interactions thanks to a bond order term in the functional form, and the environment-dependent inter-atomic potential[25] (EDIP), more recent and designed specifically for simulating defects.

To deform the system, stress increments of 1.5 GPa (equivalent to a strain around 1 to 1.4% according to the stress orientation) are successively applied, the atomic positions being relaxed between each increment. Two relaxation techniques are used. Either, a static relaxation with a conjugate gradients algorithm is performed, until forces on atoms are smaller than 10^{-3} eV/Å, or temperature is introduced in simulations[26] with molecular dynamics, in order to investigate its effect on the nucleation. After an initial static relaxation with conjugate gradients, temperature is introduced by increment of 300K, with a simulation time ranging from 5 to 50 ps.

III. RESULTS WITH THE STILLINGER-WEBER POTENTIAL

Three temperature domains have been considered; the first one at 0K, the second one for low temperatures ($\lesssim$ 900K) and the last one for high temperatures ($\gtrsim$ 900K). In each case, we focused on relevant stress orientations, in particular those that increase the probability of nucleating the four possible dislocations (60°, screw, 90° and 30°). Few other stress orientations have also been checked. All results are summarized in the Table I. All the cases presented here concern systems with D_B non re-bonded surface steps. The main effect of higher steps, like cleavage ledges, is a slight decrease of the elastic limits. In addition, the plastic events remain qualitatively

similar.

A. Calculations at 0 K; effect of stress orientation

At 0K, the plastic events appear under large strains in both compression and traction, i.e. greater than 7% (10.5 GPA) (Table I). They are initiated from the surface, in the close neighborhood of the step. Note that the elastic limits for stressed systems with surface steps are always smaller than for systems without surface steps. Hence the steps help for forming plastic events, by lowering the required stress, and by confining the starting surface area. Before the occurrence of plastic events, the system is elastically deformed and the resulting shear strains are mainly located in shuffle set planes.

Investigations have been performed with stress orientations favoring the nucleation of perfect dislocations. For the 60° dislocation, the most efficient orientation is $\alpha = 22.5°$ both in traction and in compression (Fig. 1b). The results in traction show a relatively large elastic limit of 22.5 GPa (18.7%). Beyond this stress, plasticity occurred and the relaxed system is displayed in the Fig. 4. The insert at the top of the figure clearly shows that the surface step is now twice higher. Moreover the displacements in the shuffle set plane crossing the step correspond to the slip of a 60° dislocation. On the second insert into the Fig. 4, one can see the dislocation that has stopped on the bottom of the simulation box and another 60° dislocation with the same screw component occurring in the symmetric {111} shuffle set plane from the frozen bottom. Since the dislocation is stopped on the frozen zone (which mimics the bulk) the system must find another slip system to continue its relaxation. In compression, large plastic strains appear from the surface steps for a strain of around -10% (-12 GPa), following approximately the {111} planes, but without any clearly identifiable dislocations.

The perfect dislocation in the screw orientation, should be favored by a stress disorientated at around 45° in both compression and traction (Fig. 1b). However, under a compressive stress, a 60° dislocation instead is nucleated in the shuffle set plane crossing the step. The dislocation decreases the step height and glides in the plane of the shuffle set up to the frozen bottom of the simulation box. Under a tensile stress, defects identified as micro-twins are formed from the surface step. It seems that these defects are due to a peculiar behavior of the SW potential when the resolved shear stress in the {111} planes is along the anti-twinning direction. A previous analysis has shown that these twins are formed by glides in two shuffle set planes with a rotation of trimers in the glide set plane.[27] In Brief, in both cases traction and compression, no screw dislocation has been nucleated.

Then, to nucleate partial dislocations, calculations with the most efficient stress orientations are performed. When a non disorientated tensile stress favoring the 90° partial is applied on the system (Fig. 1b), the relaxation of the atomic positions leads to the crystal fracture. The crack is formed from the surface step for a stress of 31.5 GPa (22.9%).

The 30° partial dislocation is privileged by a compressive stress with an angle of 36°. Instead, a perfect 60° dislocation is nucleated in the plane of the shuffle set crossing the surface step. Finally, although the stress orientations are ideal to form partial dislocation according to the Schmid factor, none is nucleated.

We have also checked several other configurations. In particular, stress orientations favoring anti-twinning configurations, one for $\alpha = 0°$ in compression and another for $\alpha = 36°$ in traction. It appeared that for both cases, micro-twins are nucleated from the surface steps, what may be attributed to a somewhat odd behavior of the SW potential. In some cases, for a tensile stress and $\alpha = 36°$, we obtained peculiar glide events after deformation. In particular, considering a ledge and not a single step, the structure examination after relaxation revealed the presence of a 60° and a screw dislocations. We have also investigated a system under tension and a disorientation angle $\alpha = 10°$, for which the resolved shear stresses on the 90° and the 60° dislocation are the same (Fig. 3). The result is equivalent to the situation of a non-disorientated tensile stress, with the fracture of the crystal.

So it appears that at 0K, in spite of the many stress orientations tested, only perfect dislocations, especially 60°, located in the shuffle set plane passing through the surface step are nucleated. No dislocations in the glide set planes have been obtained.

B. Other temperatures

The same stress orientations have also been studied in the low temperature domain. The main difference with the 0K study is the lowering of the elastic limit as the temperature increases in both traction and compression. However, the results remain qualitatively similar to what has been found at 0K. Only perfect 60° dislocations are routinely nucleated. And no dislocation has been formed in the glide set plane. Nevertheless, few differences have to be noted. Under a compressive stress favoring the 60° dislocation, i.e. at $\alpha = 22.5°$, the ill-defined plastic strains obtained at 0K are replaced by a 60° dislocation nucleated in the shuffle set plane. In another case, for a stress orientation leading to a resolved shear stress in the anti-twinning direction, i.e. at $\alpha = 36°$ in traction, the simultaneous formation of the 60° and screw dislocation is replaced by large strained zones near the surface step. These deformations look like a local phase change. The last difference is obtained with a tensile stress disorientated at about 10° for which the resolved shear stresses on the 90° and 60° dislocations are the same. Our results show the nucleation of a 60° dislocation in the shuffle set plane crossing the step. The dislocation glides a distance around 15 Å before leading to the fracture of the crystal.

For the high temperature domain, the elastic limits continue to decrease as the temperature is raised. No dislocation in the planes of the glide set is observed. However the stress in the system is now relaxed in a new manner. Previously, at low temperature, the glide events were relatively frequent in the plane of the shuffle set. Now at high temperatures, the glide events in the shuffle set planes become more and more rare as the temperature increases, until they totally disappear. Instead, they are replaced by disorder in the surface along the step line looking like amorphization zones and often close to the steps.

IV. RESULTS WITH THE TERSOFF POTENTIAL AND EDIP

The results obtained with the SW potential have shown that only perfect 60° dislocations are nucleated in the shuffle set plane, and at low temperature. A previous study on bulk silicon has shown that the Tersoff potential and EDIP are less reliable than SW in the case of large shear.[28] We have restricted the investigations using these potentials to the stress orientations favoring the nucleation of a 60° dislocation, i.e. with a tensile or compressive stress at $\alpha = 22.5°$.

The calculations done with the Tersoff potential at 0K give very large elastic limits. They are around 46.7% (51 GPa) and -38.5% (-42 GPa) under tensile and compressive stress, respectively. In traction, the crystal periodicity along the step line direction is lost due to large strains of the bulk looking like the beginning of a phase transition (Fig. 6a), leading sometimes to a crystal crack from the surface near the step. In compression, up to -22%, the strains remained homogeneous. Then slight undulations appeared on the surface up to -37%. Finally, a plastic strain occurred in the (011) planes close to the surface step (Fig. 6b). In all cases no glide events are observed.

Calculations have been performed at different temperatures and several applied stresses. The only effect is the decrease of the elastic limits and the expansion of plastic strains. However, using high steps (cleavage ledges), a large compressive strain (-11%) and very high temperatures ranging from 1200K to 1500K, we managed to nucleate 60° dislocations in the shuffle set plane passing through the step edge (Fig. 5b).

The calculations performed with EDIP at 0K also show much larger elastic limits than the ones obtained with SW. They are around 34.5% (52.5 GPa) in traction and -8.9% (-13.5 GPa) in compression. Under tensile stresses, a crystal crack occurred, while under compressive stresses, the {111} shuffle set plane passing through the step edge is largely sheared (Fig. 6c-d). This shear propagates from the surface to the slab bottom without dislocation. When the applied strain increased neighboring shuffle set planes are also sheared.

V. DISCUSSIONS

A. Dependency on the potentials

Although the same stress orientations have been checked, at 0K and non zero temperature, the results are often different from one potential to another. In order to establish which potential represents best sheared silicon, we have recently compared these three potentials with ab initio methods.[28] A homogeneous shear is imposed on {111} planes in a $< 110 >$ direction, the amplitude of shear goes up to 122% where the diamond cubic structure is recovered. At each shear value, the system is relaxed in order for the simple FCC two sublattices forming the diamond structure to reach their relative equilibrium position. In this way, one sees how the imposed shear is distributed in the glide set and the shuffle set respectively. When the full amplitude of the imposed shear has been applied, the crystal structure returns to perfect diamond cubic with the SW potential and EDIP, as well as in the ab initio calculation, through a bond breaking and new bond formation across the shuffle plane. However, such a bond switching is not observed with the Tersoff potential which in these conditions, does not appear suitable for describing dislocation nucleation.

When comparing the energy curves of bulk silicon as a function of the homogeneous shear strain. Only the curve of the SW potential is relatively smooth with a shape and amplitude similar to the one calculated in DFT-LDA. The Tersoff curve is discontinuous and the EDIP curve exhibits an angular point. Thus, only SW can account for the atomic surrounding without energy discontinuity when the crystal is largely strained. This feature is even more marked when looking at derivative quantities, related to stresses. In addition, critical values such as the theoretical shear strength are overestimated by a factor of about two with the Tersoff potential and EDIP compared to the DFT calculation, whereas Stillinger-Weber is much closer to ab initio.

Concerning EDIP, it has not been possible to use this potential at the large strains considered here because of an accident occurring in the curve energy versus shear strain which produces a shear instability of the crystal. The SW potential is not exempt of drawbacks. When the crystal is sheared in the anti-twinning direction,[27] twinning is produced through shearing in the shuffle set planes. We do not think that this prevents the use of the SW potential for the other stress orientations.

Hopefully, there are indications that these inadequacies of the potentials may become less important at high temperatures, where dislocations can be formed at lower imposed strains. For example, under a compressive stress with $\alpha = 22.5°$, the twin-like defect created by the SW artefact, is replaced by a 60° dislocation at a smaller strain. Another example is given by the Tersoff potential

which at high temperature and for large step height can lead to the formation of a 60° dislocation. Temperature may rub out unphysical irregularities in the potentials.

B. Role of the surface step

Here, we focus on the results obtained with the SW potential. Plasticity occurs for very large strains, somewhat smaller in compression than in tension. Although the particular crystal structure and potential may be important, one must consider that at the very large stresses considered here,the solid may undergo some buckling instability of course in compression and not in tention, instability which helps dislocation formation. Others studies are in progress to clarify this point.

For bulk silicon, The theoretical strengths obtained with The Stillinger-Weber potential are large, in agreement with ab initio calculations Roundy and M.L. Cohen.[29] Indeed, the limits of elasticity of the systems with a free surface presenting steps are definitely smaller than without step. For example at 0K, for a non disorientated stress, in tension (in compression) the yield strain is about 22.9% (-7.6%) with surface steps and about 28.3% (-11%) without surface step respectively. Generally the plastic strains, such as fracture, the glide events or the amorphization zones..., occur from the steps or from their immediate neighborhood. In fact the presence of the step breaks the symmetry of the system leading to some stress localization near the step. Thus the surface step is a privileged site for plasticity.

C. Slip system: glide or shuffle

Now, we discussed whether the dislocation nucleation occurs in the glide or in the shuffle set planes, using the results obtained with the SW potential.

In principle, the perfect 60° and screw dislocations can be formed in either the glide or the shuffle plane, but in our results, the dislocations are nucleated only in the planes of the shuffle set. The simulation with the stress orientation most appropriate for nucleating 90° and 30° partials in the glide set, lead to the fracture of the crystal and to the formation of a 60° dislocation in the shuffle set, respectively. This result is consistent with the fact that for a slip in the shuffle set, only one covalent bond must be broken compared to three in the glide set.[30]

In the high temperature domain, the probability of dislocation nucleation tends to drop and plastic strains taking the form of amorphizations occur. As temperature is raised, the strain at which some plasticity occur, decreases and this process lasts until the thermal vibrations are sufficient to begin the melting/amorphisation and the applied strains to small to initiate a dislocation in the shuffle set. Here again, no dislocation is formed in the glide set. Conversely to our simulations, at high temperature, the observed dislocations are partial dislocations belonging to the glide set planes. It is commonly accepted that they move more easily through the nucleation and propagation of double kinks thanks to thermal vibrations.[19,31,32,33] However, the size of the simulation cell along the dislocation line used here, 4 a/2< 110 >, is too small to allow the formation of a kink pair. Consequently, only two plastic events are possible in the simulation: the nucleation of an infinite straight 60° dislocation in the shuffle set planes or amorphisation/melting, depending on the temperature.

Experimentally, the observations done in both low and high temperature domains reveal a slip mode transition depending on the temperature. At low temperature dislocations seem to glide in the shuffle set planes and at high temperature in the glide set planes.[7,34,35] Whatever the temperature, our simulations have shown that the nucleation of straight dislocation in the glide set plane is not allowed due to geometric reasons. The only type of dislocation, the 60°, is nucleated in the shuffle set planes. Moreover we have observed that high temperatures prevent the dislocation formation in this set. Thus our results are not in disagreement with the experimental facts, but complementaries calculations in 3 dimensions, in order to allow the kink propagation, are necessary to confirm the slip mode transition.

D. Character of the dislocation nucleated.

In order to understand the kind of dislocation formed, we tried to establish the main criteria that govern this choice. Usually, when a crystal is stressed, the slip system with the largest resolved shear stress along the Burgers vector **b** is favored. In our case, the resolved shear stress on each dislocation, proportional to the Schmid factor, is directly related to the stress orientation α. In the range of temperature where the glide events are frequently observed for the SW potential, in most cases, the plastic events are consistent with the results predicted by the Schmid factors. For example, on the Figure 1b, the 60° dislocation is favored for a stress orientation $\alpha = 22.5°$ in traction and in compression, what is obtained in our simulations. One sees from the same figure, that a compressive stress disorientated by 36° favors the 30° partial, that is a strain in the twinning sense. Since dislocations of the glide set are not activated, as explained above, the system finds another slip system to relax the applied stress. In these conditions of twinning, two dislocations are possible the 60° and the screw. In our simulations, the dislocation nucleated is the 60°, i.e. the one with the largest Schmid factor (Fig. 3).

However several cases cannot be explained on the basis of the Schmid factor only, the character of the dislocation must also be taken into account. For example, under a non disorientated tensile stress favoring the twinning stress along the $\mathbf{b}_{90°}$ partial (Fig. 1b), a crystal crack is produced without glide events. Following the Schmid

factor analysis, two 60° on both sides of the partial dislocation could then be nucleated. But the resolved shear stress along both symmetric $< 110 >$ directions (Fig. 3) are equal, what may prevent the choice of one slip system. To check this, a calculation with a stress orientation at 10° that breaks the symmetry of the problem, has formed a 60° dislocation in agreement with the Schmid factor.

Compare this case to that where the stress orientation is disorientated by 45° (Fig. 3 curves 3 and 5). Although the resolved shear stress is the same on the screw and the 60°, the latter is nucleated, in compression. It is worth remarking that the two types of dislocations have different mobility properties, cf. for instance the Peierls stresses. The calculations performed with the SW potential have shown that the Peierls stress on the 60° dislocation is smaller than on the screw.[36] To relax the applied stress, the nucleation of a perfect 60° dislocation is then favored.

The other discrepancies between the Schmid factor analysis and the simulation results are mainly due to the unphysical defect created by the SW potential, the microtwins, which pollute largely the results in both traction and compression, when the applied stress acts in the antitwinning sense. For example in compression at 0K, the micro-twin formation disappears as the stress orientation α increases. Hence the resolved shear stress along the anti-twinning direction must be as small as possible to avoid this kind of defects.

The analysis of the plastic strains as a function of the stress orientation shows that the character of the dislocations nucleated from surface steps can be mainly predicted by examining the Schmid factor and the Peierls stress. Other factor may play a role, though. For example, the crystal symmetry may prevent the choice of one particular slip system leading to fracture.

VI. CONCLUSION

We have investigated the nucleation of dislocations from linear surface defects such as steps, when the system is submitted to a uniaxial stress. Although the elastic limits remain relatively close to the theoretical strength, it appears that the surface steps weaken the atomic structure and help the formation of glide events like dislocations. The glide evens are nucleated and propagated in the planes of the shuffle set. No straight dislocation is formed in the glide set plane. The geometry of the simulation cell used here which prevents the formation of kink pairs, does not allow for the expected formation of partial dislocations in the shuffle set at high temperature.

In addition, we have remarked that the high temperature decreases the probability of nucleating perfect dislocation in the shuffle set plane. Melting/amorphisation of silicon occurs before reaching the required shear stress to initiate the dislocation. These results seem consistent with the assumption that at low temperature the dislocations glide in the planes of the shuffle set, based on the observation of non dissociated dislocations in silicon samples deformed at low temperature in conditions preventing failure.[7,35] Supplementary studies are planned to check the nucleation of dislocation loops in the glide set planes with high temperature.

The role of the stress orientation on the nucleated defects has been studied from the calculations performed with the SW potential. Although the results are slightly biased by the somewhat unphysical defect produced by the SW potential when the stress acts in the antitwinning direction, it emerges that the type of dislocation nucleated is chosen by the resolved shear stress and the Peierls stress.

Concerning the empirical potentials, it has not been possible to nucleate any dislocations in the simulations performed with the Tersoff potential and EDIP at 0K. The Tersoff potential has too high energy barriers preventing the bond breaking required to nucleate a dislocation at low temperatures. While EDIP presents a shear instability in the shuffle set planes. With the Tersoff potential, the overcoming of the energy barriers leading to the dislocations nucleation has become possible at high temperature. By extrapolation, EDIP is probably able to nucleate dislocations thanks to the thermal vibrations. To summarize, although the different results are potential-dependent, only the simulations performed with the SW potential can be taken into account at 0 K as demonstrated in our previous study on bulk system. Actually, we are trying a similar calculation with ab initio methods on a relatively large system. A calculation with a small system of about 200 atoms has already produced the nucleation of a 60° perfect dislocation in the shuffle set.

* Electronic address: julien.godet@etu.univ-poitiers.fr

[1] A. Moulin, M. Condat, and L. P. Kubin, Phil. Mag. A **79**, 1995 (1999).

[2] J. Dunstan, J. Mater. Sci.: Materials in Electronic **8**, 337 (1997).

[3] S. C. Jain, A. H. Harker, and R. A. Cowley, Phil. Mag. A **75**, 1461 (1997).

[4] R. X. Wu and G. C. Weatherly, Phil. Mag. A **81**, 1489 (2001).

[5] Y. Q. Wu and Y. B. XU, Phil. Mag. Lett. **78**, 9 (1998).

[6] C. Scandian, H. Azzouzi, N. Maloufi, G. Michot, and A. George, Phys. Stat. Sol. **171**, 67 (1999).

[7] J. Rabier, P. Cordier, J. L. Demenet, and H. Garem, Mater. Sci. Eng. A **A309-A310**, 74 (2001).

[8] M. Ichimura and J. Narayan, Mater. Sci. Eng. B **31**, 299 (1995).

[9] A. Aslanides and V. Pontikis, Phil. Mag. Lett. **78**, 377 (1998).

[10] Y.-M. Juan, Y. Sun, and E. Kaxiras, Phil. Mag. Lett. **73**, 233 (1996).

[11] H. Gao, C. S. Ozkan, W. D. Nix, J. A. Zimmerman, and L. B. Freund, Phil. Mag. A **79**, 349 (1999).
[12] G. Xu, A. S. Argon, and M. Ortiz, Phil. Mag. A **75**, 341 (1997).
[13] B. J. Gally and A. S. Argon, Phil. Mag. A **81**, 699 (2001).
[14] A. S. Argon and B. J. Gally, Scripta Materialia **45**, 1287 (2001).
[15] S. Brochard, P. Beauchamp, and J. Grilhé, Phil. Mag. A **80**, 503 (2000).
[16] S. Brochard, P. Beauchamp, and J. Grilhé, Phys. Rev. B **61**, 8707 (2000).
[17] T. W. Poon, S. Yip, P. S. Ho, and F. F. Abraham, Phys. Rev. B **45**, 3521 (1992).
[18] J. Godet, L. Pizzagalli, S. Brochard, and P. Beauchamp, Scripta Materialia **47**, 481 (2002).
[19] J. P. Hirth and J. Lothe, *Theory of dislocations*, 2nd (Wiley, 1982).
[20] D. J. Chadi, Phys. Rev. Lett. **43**, 43 (1979).
[21] A. Ramstad, G. Brocks, and P. J. Kelly, Phys. Rev. B **51**, 14504 (1995).
[22] D. J. Chadi, Phys. Rev. Lett. **59**, 1691 (1987).
[23] F. H. Stillinger and T. A. Weber, Phys. Rev. B **31**, 5262 (1985).
[24] J. Tersoff, Phys. Rev. B **39**, 5566 (1989).
[25] M. Z. Bazant, E. Kaxiras, and J. F. Justo, Phys. Rev. B **56**, 8542 (1997).
[26] J. Rifkin and jon.rifkin@uconn.edu, *Xmd - molecular dynamics program, www.ims.uconn.edu/centers/simul/♯software* (1999).
[27] J. Godet, L. Pizzagalli, S. Brochard, and P. Beauchamp, to be published. **0**, 0 (2003).
[28] J. Godet, L. Pizzagalli, S. Brochard, and P. Beauchamp, J. Phys.: Condens. Matter **15**, 6943 (2003).
[29] D. Roundy and M. Cohen, Phys. Rev. B **64**, 212103 (2001).
[30] W. Shockley, Phys. Rev. **91**, 1563 (1953).
[31] V. V. Bulatov, S. Yip, and A. S. Argon, Phil. Mag. A **72**, 453 (1995).
[32] V. V. Bulatov, J. F. Justo, W. Cai, S. Yip, A. S. Argon, T. Lenosky, de Koning M., and D. de la Rubia T., Phil. Mag. A **81**, 1257 (2001).
[33] T. E. Mitchell, P. M. Anderson, M. I. Baskes, S. P. Chen, R. G. Hoagland, and A. Misra, Phil. Mag. **83**, 1329 (2003).
[34] M. S. Duesbery and B. Joós, Phil. Mag. Lett. **74**, 253 (1996).
[35] J. Rabier and J. L. Demenet, Scripta Materialia **45**, 1259 (2001).
[36] Q. Ren, B. Joos, and M. S. Duesbery, Phys. Rev. B **52**, 13223 (1995).

Table captions

Table I

Figure captions

TABLE I: Summary of plastic events obtained with the SW potential, for several stress orientations at 0K and with temperature. All the glide events are localized in the shuffle set planes. The elastic limits are given at 0K by the uniaxial stresses. Note that, the strains along the stress direction are obtained by the linear elasticity.

α	Stress (GPa)		strain (%)	Results T = 0K	T $\lesssim$ 900K
0°	Trac	31.5	22.9	fracture	fracture
	Comp	−10.5	−7.6	micro-twin	micro-twin
10°	Trac	25.5	19.1	fracture	perfect 60° then fracture
	Comp	−10.5	−7.9	micro-twin	micro-twin
22.5°	Trac	22.5	18.7	perfect 60°	perfect 60°
	Comp	−12.0	−10.0	plastic deformations in {111} planes	perfect 60°
36°	Trac	21.0	19.2	micro-twins + sometime 60° and screw	micro-twins + large strained zone
	Comp	−13.5	−12.4	perfect 60°	perfect 60°
45°	Trac	21.0	19.7	micro-twins	micro-twins
	Comp	−15.0	−14.0	perfect 60°	perfect 60°

FIG. 1: Diamond-like structure projected along $[0\bar{1}1]$ (a) and along [111] (b). All the possible slip directions following the Burgers vectors of the 60°, 90°, 30° and screw dislocations are considered. For each dislocation, the best stress orientation giving the maximum resolved shear stress is noted.

FIG. 2: Calculation cell with a D_B step non re-bonded. $\boldsymbol{\sigma}$ is the applied uniaxial stress and α the angle between the [011] normal step and the stress direction.

FIG. 3: The Schmid factors versus the stress orientation α are drawn for five slip directions; two along the Burgers vectors of the 60°, $< 10\bar{1} >$ (1) and $< 1\bar{1}0 >$ (3), two along the Burgers vector of the partials, $< 2\bar{1}1 >$ for the 90° (2) and $< 1\bar{2}1 >$ for the 30° (4) and the last one along $\mathbf{b}_{screw}$, $< 0\bar{1}1 >$ (5), parallel to the step line. (the Schmid factor being proportional to the resolved shear stress).

FIG. 4: Nucleation of a perfect 60° dislocation from the surface step, in a plane of the shuffle set with the SW potential. The tensile strain is about of 18.7% and disorientated of 22.5°.

FIG. 5: Nucleation of a perfect 60° dislocation in the shuffle set plane thanks to the temperature. The compressive stress is disorientated of 22.5°. (a) SW: the D_B step disappears for a strain of -7.5% at 900K, (b) Tersoff: one atomic layer disappears for a strain of -11.0% at 1200K.

FIG. 6: Snapshot of silicon structure close to the elastic limit with a stress disorientated of 22.5°. (a) Tersoff with a strain of 46.7%, (b) Tersoff with a strain of -38.5%, (c) EDIP with a strain of 34.5%, (d) EDIP with a strain of -8.9%.

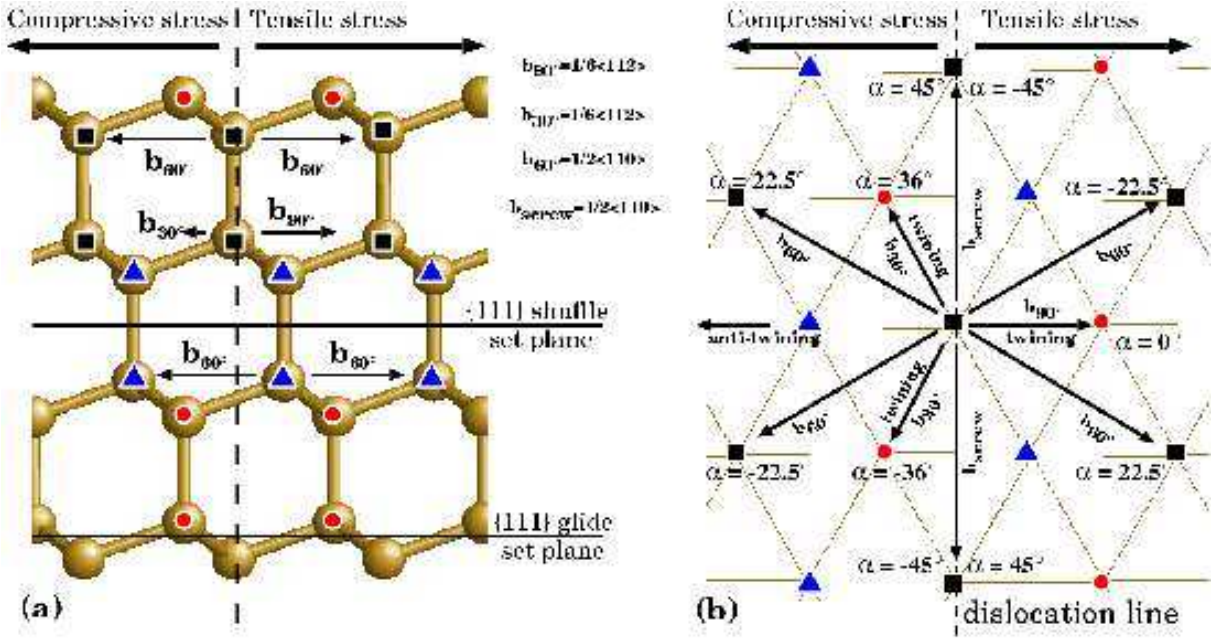

Figure 1

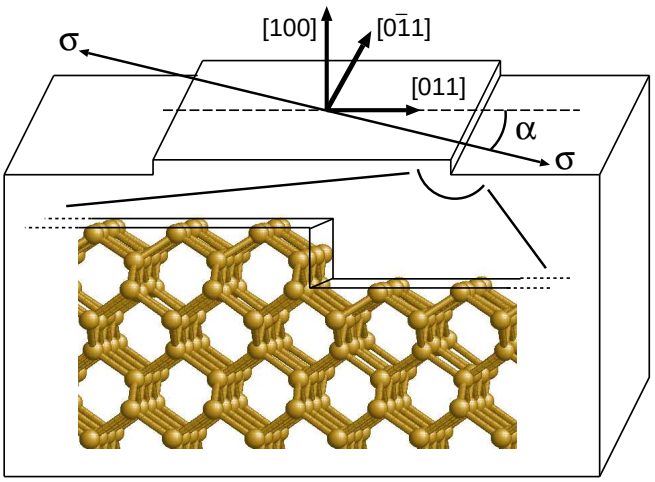

Figure 2

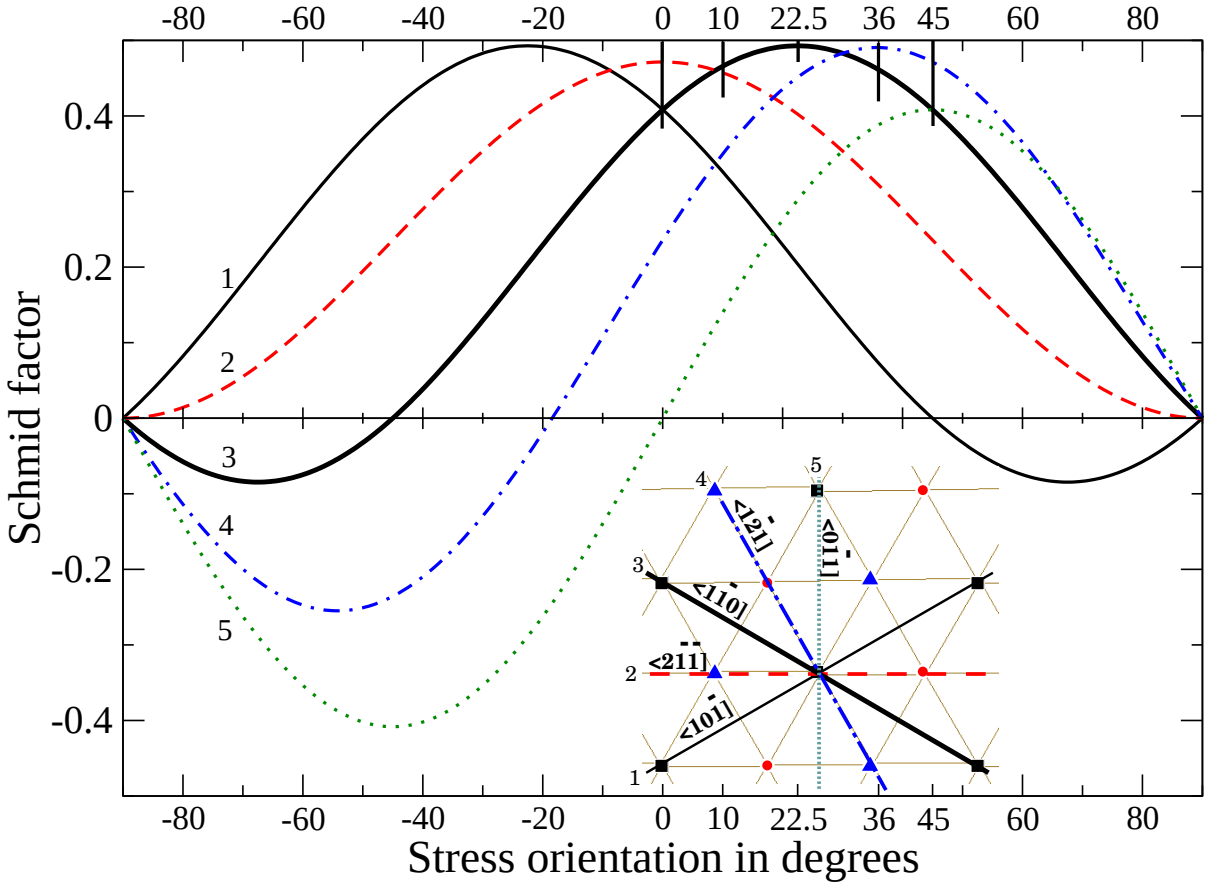

Figure 3

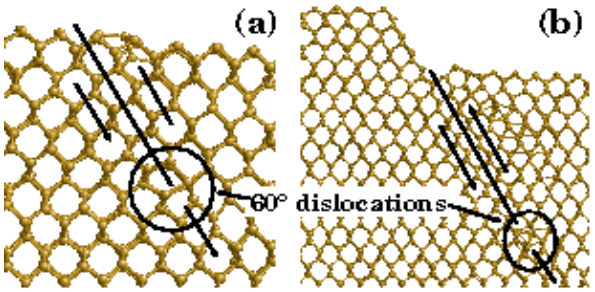

Figure 5

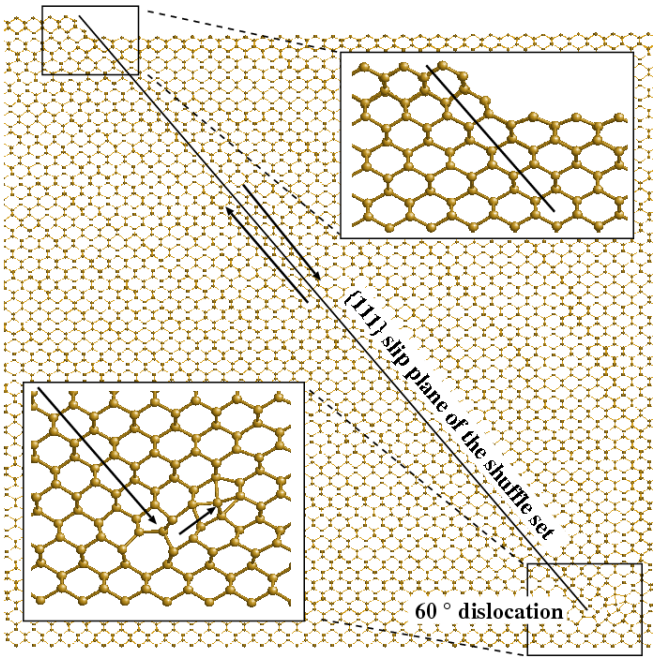

Figure 4

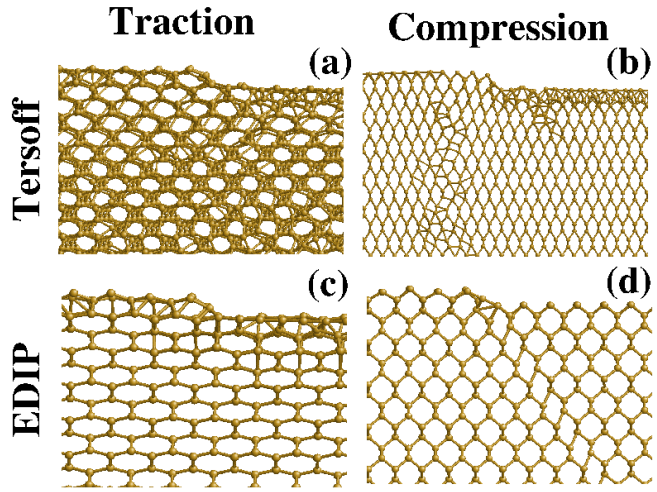

Figure 6